Meteorol. Atmos. Phys. 58, 193–203 (1996)

Meteorology and Atmospheric Physics

[1] Supercomputer Computations Research Institute, Florida State University, Tallahassee, Florida, U.S.A.
[2] Department of Mathematics and SCRI and GFDI, Faculty Associate, Florida State University, Tallahassee, Florida, U.S.A.

The Linearization and Adjoint of Radiation Transfer Processes in the NMC Spectral Model Part I: Solar Radiative Transfer

J. Zou[1] and **I. M. Navon**[2]

With 5 Figures

Received August 10, 1994
Revised December 22, 1994

Summary

Linearization and adjoint-model derivation for the solar radiation transfer codes in the NMC spectral model have been carried out. Verification of the validity of resulting tangent linear model and the correctness of the corresponding adjoint have been performed. Applications of derived adjoint model are considered, including parameter estimation for inputs to solar radiation codes with aid of the physics (i.e., the solar radiation codes) and a sensitivity study of the downward solar radiation flux at the earth surface with respect to water vapor amount at various heights.

1. Introduction

Variational data assimilation (VDA) with the NMC global spectral model has become increasingly sophisticated in recent years as reviewed by Zou and Navon (1994a). Navon et al. (1992) carried out VDA with an adiabatic version of NMC spectral model using model-analyzed data, followed by Zou et al. (1993a) where control of gravitational oscillation was enforced in the same model. Zou et al. (1993b) have taken into account moisture processes such as the large-scale precipitation and cumulus convection in their VDA. Recently, Zou et al. (1994b) have used direct observations operationally available at NMC in a comprehensive 4-D VAR framework, including a background term in the cost functional. The covariance statistics were obtained from the 3-D VAR SSI (spectral statistics interpolation) (cf., Derber et al., 1991; Parrish and Derber, 1992; Derber et al., 1993; Wu and Derber, 1994; Derber et al., 1994). Yet the adjoint of the largest physics package in the NMC spectral model, namely, the radiative transfer process, remains to be derived and included for carrying out either 4-D VDA, parameter estimation or sensitivity analysis with the NMC spectral model.

It is in view of this that we focus here our attention on developing the tangent linear model and adjoint of radiative transfer codes in the NMC spectral model with a view towards the aforementioned applications. This paper reports only a part of the effort in this direction, that is, solar radiative transfer, while results from ongoing research on terrestrial radiative transfer will be reported in a follow-up paper.

The remainder of this paper is organized as follows. Section 2 reviews parameterized solar radiative flux calculations in the NMC spectral model. Section 3 presents derivation of linear tangent model and its corresponding adjoint, while Section 4 provides examples of application including sensitivity study and parameter estimation with aid of the physics. Finally, a summary and discussion are presented in Section 5.

2. Flux Calculations in the NMC Spectral Model

This section aims at describing the solar radiative flux calculation in the NMC spectral model in a form more transparent to subsequent development of the tangent linear and corresponding adjoint models (See Campana et al., 1988 and references therein for details).

Let a model atmosphere be divided vertically into L homogeneous layers indexed downwards with top of the atmosphere as $l=1$ and the earth surface as $l=L+1$ (Note that the vertical indexing here is in an opposite direction to that of NMC spectral model). Consider a beam of solar radiation traversing through the l-th layer. Denote downward and upward fluxes at l-th layer interface by F_l^+ and F_l^-, respectively. To calculate F_l^+ or F_l^-, consider a solar radiation beam illuminating from above and diffusively transmitted through a composite of layers 1 through $l-1$. Transmission function at bottom of the composite layer, i.e., at l-th layer interface, is given by

$$T_{1,l}^{\pm} = T_{1,l}^{O_3}\, T_{1,l}^{H_2O}\, T_{1,l}^{C_2O} \tag{1}$$

where the superscripts indicate absorbers i.e., ozone, water vapor and carbon dioxide respectively, for their related transmission functions. Parameterized forms of these transmission functions are given respectively by

$$\begin{aligned} T_{1,l}^{O_3} &= 1 - 0.02118u_l^{\pm}(O_3)/(1 + 0.042u_l^{\pm}(O_3) \\ &\quad + 0.000323u_l^{\pm}(O_3)^2) \\ &\quad + 1.082u_l^{\pm}(O_3)/(1 + 1.1386u_l^{\pm}(O_3))^{0.805} \\ &\quad + 0.0658u_l^{\pm}(O_3)/(1 + (103.6u_l^{\pm}(O_3))^3) \end{aligned} \tag{2}$$

$$T_{1,l}^{H_2O} = \exp(-\tau_l^{\pm}(H_2O)),$$

$$\tau_l^{\pm}(H_2O) = \min(\tau_C, k_n u_l^{\pm}(H_2O)) \tag{3a, b}$$

$$\begin{aligned} T_{1,l}^{C_2O} &= 1 - 0.00235(u_l^{\pm}(CO_2) + 0.0129)^{0.26} \\ &\quad - 7.58265 \times 10^{-4}. \end{aligned} \tag{4}$$

In the above τ_C is a critical value of the optical path for water vapor obsorber, and the quantity, $u_l^+(H_2O)$ for example, is the effective water vapor amount traversed by the direct solar radiation in reaching the l-th level and calculated as pressure weighted integral of H_2O mixing ratio $q(H_2O)$

$$u_l^+(H_2O) = M \sum_{j=1}^{l-1} (\bar{p}_j/p_s) q_j(H_2O) \Delta p_j \tag{5}$$

where M, a function of solar zenith angle, accounts for the slant path and refraction, $\bar{p}_j$ is the mean pressure of the j-th layer, p_s the surface pressure, and Δp_j the pressure interval of the layer. The weighting factor $(\bar{p}_j/p_s)$ accounts for the pressure broadening effect on water vapor absorption spectrum. $u_l^+(O_3)$ and $u_l^+(CO_2)$ are defined similarly except for absence of the pressure weighting in case of O_3.

The "–" sign in (1)–(5) applies to the case where diffuse solar radiation illuminates the composite layer from below. In this case the effective absorber amount traversed by the reflected radiation in reaching the l-th level from below, $u_l^-(H_2O)$ in (3) for example, is given by

$$\begin{aligned} u_l^-(H_2O) &= u_{L+1}^+(H_2O) \\ &\quad + \bar{M} \sum_{j=L+1}^{l} (\bar{p}_j/p_s) q_j(H_2O) \Delta p_j \end{aligned} \tag{6}$$

where $\bar{M}$ is the effective magnification factor for diffuse upward radiation.

For a clear sky, fluxes F_l^+ are F_l^- are readily obtained from

$$F_l^+ = T_{1,l}^+ \tag{7}$$

$$F_l^- = R_1 T_{1,l}^-(T_{1,L+1}^-) \tag{8}$$

where R_1 represents combined effect of the surface albedo and the effective albedo of the low atmosphere as a reflecting region for the O_3 absorption band, but reduces to the surface albedo for other bands. Note that fluxes are expressed here in units of F_1^+, the incident solar flux density at TOA.

For a cloudy sky, consider a system of parallel-plane clouds indexed upwards with the earth surface as the first cloud (i.e., $k=1$) and its transmission function $T_1^{ClO}=0$. Here the superscript ClO refers to cloud. Consider two layer of clouds indexed as k and $k-1$, one on top of the other. Let $T_{lt(k-1)}^C$ be the transmissivity between top of k-th cloud layer and top of $(k+1)$-th cloud with k-th cloud transmissivity T_k^{ClO} included, and $T_{lt(k-1)}$ be the transmissivity due to gaseous absorbers in the region between the two clouds. Then in terms of T^+, we have

$$T_{lt(k-1)}^C = T_k^{ClO}(T_{1,lt(k-1)}^+ / T_{1,lt(k)}^+) \tag{9}$$

$$T_{lt(k-1)} = T_{1,lt(k-1)}^+ / T_{1,lb(k)}^+ \tag{10}$$

where the subscript $lt(k)$ [or $lb(k)$] is layer index l for top [or bottom] of the k-th cloud. For the

fluxes at top of $(k-1)$-th cloud, the following recursive relations hold

$$F^-_{lt(k-1)} = F^-_{lt(k)}\alpha^C_k/(\alpha_k T^C_{lt(k-1)}) \tag{11}$$

$$F^+_{lt(k-1)} = F^-_{lt(k-1)}/\alpha_k \tag{12}$$

for $k = K, K-1, \ldots, 1$, with the fluxes at top of the atmosphere (TOA) given by

$$F^-_{lt(K)} = \alpha_K T^+_{1,lb(K)} \tag{13}$$

$$F^+_{lt(K)} = T^+_{1,lb(K)} \tag{14}$$

The quantity α_k in the above is determined upwards from

$$\alpha_k = \alpha_{k-1} T^C_{lt(K-1)}/(1 - \alpha_{k-1} R^{ClO}_k T_{lt(k-1)}{}^2) + R^{ClO}_k \tag{15}$$

with $\alpha_1 = R^{ClO}_k$; α^C_k is obtained as $\alpha_k - R^{ClO}_k$.

For the fluxes F^+_l and F^-_l at levels intermediate between the two layers of cloud, i.e., for $lb(k) \leqslant l \leqslant lt(k-1)$

$$F^+_l = F^+_{lt(k-1)}(T^+_{1,l}/T^+_{1,lt(k-1)}) \tag{16}$$

$$F^-_l = F^-_{lt(k-1)}(T^-_{1,l}/T^-_{1,lt(k-1)}) \tag{17}$$

Finally, to obtain the fluxes inside a thick cloud (i.e., consisting of at least two model layers), say the k-th cloud, it is assumed that solar radiation heating rate within the cloud is a constant. This allows calculation of F^+_l and F^-_l from a linear interpolation of the fluxes at top and bottom of the cloud

$$F^+_l = F^+_{lt(k)} + \beta_{lk}(F^+_{lt(k)} - F^+_{lb(k)}) \tag{18}$$

$$F^-_l = F^-_{lt(k)} + \beta_{lk}(F^-_{lt(k)} - F^-_{lb(k)}) \tag{19}$$

for $lt(k) \leqslant l < lb(k)$, where $\beta_{lk} \equiv (p_l - p_{lt(k)})/\Delta p_k$ and p_l is the pressure at l-th level.

Note that the multiplication in (1) accounts for the overlap of ozone and water vapor absorption in the ultraviolet part of the solar spectrum (i.e., for band 1) and the overlap of water vapor and carbon dioxide in the near infrared region (i.e., for the remaining 11 bands). Also note that the flux calculations outlined above apply to individual band and a summation over the total of 12 bands is required to obtain a solar radiative flux. For further discussions readers are referred to Campana et al. (1988), or to Lacis and Hansen (1974) for absorption of solar radiation by O_3 and H_2O and to Sasamori et al. (1972) for C_2O absorption, respectively.

3. Tangent Linear Model and its Adjoint

3.1 The Tangent Linear Model (TLM) of the Solar Radiation Codes

The radiation fluxes as given by Eqs. (7)–(19) are nonlinear expressions in the model state vector, specifically in water vapor mixing ratio $\mathbf{q}(H_2O)$, due to exponential nature of the transmission functions (cf. (3)). To derive the TLM of the solar radiation codes, let us perturb water vapor mixing ratio $\mathbf{q}$, a prognostic variable of the NMC spectral model, by an amount $\delta\mathbf{q}$ (hereafter "H_2O" is suppressed for the sake of simplicity of notation). Consider resulting perturbation in fluxes $\delta\mathbf{F}^\pm$, $\mathbf{F}^\pm \equiv [F^+_1, F^-_1, F^+_2, F^-_2, \ldots, F^+_{L+1}, F^-_{L+1}]^T$. Taking a Taylor expansion of $\mathbf{F}^\pm(\mathbf{q} + \delta\mathbf{q})$ truncated to first order in $\delta\mathbf{q}$, one can write the tangent linear model as

$$\delta\mathbf{F}^\pm = (\partial\mathbf{F}^\pm/\partial\mathbf{q})\delta\mathbf{q} \tag{20}$$

where $(\partial\mathbf{F}^\pm/\partial\mathbf{q})$ denotes the Jacobian matrix of $\mathbf{F}^\pm$ with respect to $\mathbf{q}$ evaluated at the unperturbed state. As evidenced in Eqs. (7)–(19), dependence of $\mathbf{F}^\pm$ on $\mathbf{q}$ is implicit through the transmission functions $T^\pm_{1,l}$ which in turn depend on $T^{H_2O}_{1,l}$ and then the latter depends on the effective path length $u^\pm_l(H_2O)$. Evaluation of the Jacobian matrix can be carried out as simply as

$$(\partial\mathbf{F}^\pm/\partial\mathbf{q})_\mathbf{q} = \mathscr{P}_1\mathscr{P}_2\mathscr{P}_3\mathscr{P}_4 \tag{21}$$

with

$$\mathscr{P}_1 \equiv (\partial\mathbf{F}^\pm/\partial\mathbf{T}^\pm), \quad \mathscr{P}_2 \equiv (\partial\mathbf{T}^\pm/\partial\mathbf{T}^{H_2O}),$$

$$\mathscr{P}_3 \equiv (\partial\mathbf{T}^{H_2O}/\partial\mathbf{u}^\pm), \quad \mathscr{P}_4 \equiv (\partial\mathbf{u}^\pm/\partial\mathbf{q}),$$

where each $\mathscr{P}_i$ in turn is a Jacobian matrix. In the above,

$$\mathbf{T}^\pm \equiv [T^+_{1,1}, T^-_{1,1}, T^+_{1,2}, T^-_{1,2}, \ldots, T^+_{1,L+1}, T^-_{1,L+1}]^T$$

and $\mathbf{T}^{H_2O}$ and $\mathbf{u}^\pm$ are defined similarly.

To this end, the tangent linear operator $\partial\mathbf{F}^\pm/\partial\mathbf{q}$ evaluated at an unperturbed state $\mathbf{q}$ requires evaluation of $\mathscr{P}_1$ at $\mathbf{T}^\pm$, $\mathscr{P}_2$ at $\mathbf{T}^{H_2O}$, $\mathscr{P}_3$ at $\mathbf{u}^\pm$, and $\mathscr{P}_4$ at $\mathbf{q}$, respectively. The nonlinearity of $\mathbf{F}^\pm$ in $\mathbf{T}^\pm$, as seen in (7)–(8) for the clear sky case or Eqs. (9)–(17) for the cloudy case, necessitates evaluation of $\mathbf{T}^\pm$ and hence recomputation of all quantities listed in Eqs. (2) through (6) prior to obtaining a solution of the TLM. Instead of using massive amounts of storage, we have adopted the approach of online calculation for availability of these variables about which to linearize (or to set

up operators $\mathscr{P}_l$). In terms of computational expense, clearly this amounts to nearly a factor two increase in memory and CPU time for the tangent linear model or for the adjoint, a situation typical for the adjoint formalism.

Threshold processes are common in model physics and may present a challenge to derivation of a TLM and its corresponding adjoint, while the lack of differentiability with respect to control variables can impact upon our ability to obtain the minimum of the cost function. Further discussion of impact of the minimum of the cost function. Further discussion of impact of the threshold processes on variational data assimilation may be found in Hoffman et al. (1992), Vukicevic and Errico (1993), Zupanski (1993) and Zou et al. (1993b). Two types of threshold processes are encountered in the solar radiation codes of the NMC spectral model. The first process is related to testing presence of clouds, while the other occurs in testing saturation of optical thickness for water vapor (cf. (3)). The first is of no consequence due to the fact that the cloud fractional amount is now taken as a constant parameter input. To deal with the threshold on $\tau^{\pm}(H_2O)$ in (3b), we, following Hoffman et al. (1992), write (3b) as

$$\tau_l^{\pm}(H_2O) = \begin{cases} \tau_C & \text{if } \tau_l^{\pm} \geqslant \tau_C \\ k_n u_l^{\pm}(H_2O) & \text{if } \tau_l^{\pm} < \tau_C \end{cases}$$

and execute the following codes in the TLM accordingly

$$\delta\tau_l^{\pm}(H_2O) = \begin{cases} 0 & \text{if } \tau_l^{\pm} \geqslant \tau_C \\ k_n \delta u_l^{\pm}(H_2O) & \text{if } \tau_l^{\pm} < \tau_C \end{cases}$$

One way to check performance of the linear tangent model is to see how well the perturbation in fluxes $\delta\mathbf{F}^{\pm}$ from (20)–(21) approximates the corresponding exact finite difference expression $\Delta\mathbf{F}^{\pm} \equiv \mathbf{F}^{\pm}(\mathbf{q}+\delta\mathbf{q}) - \mathbf{F}^{\pm}(\mathbf{q})$, where $\mathbf{F}^{\pm}(\mathbf{q})$ is obtained from the nonlinear solar radiation codes. Ideally one would expect that $\delta\mathbf{F}^{\pm} - \Delta\mathbf{F}^{\pm} \sim O(\delta\mathbf{q})$. A numerical verification has been carried out, where the unperturbed water vapor $\mathbf{q}$ along with ozone is prescribed by McClatchey tropical profiles (McClatchey et al., 1971) and C_2O mixing ratio is set to 5.01×10^{-4}. Solar zenith angle is taken to be 10° and the surface albedo set to 0.2. Three cloud layers are present, with details of their specification summarized in Table 1.

Figure 1 displays favourable comparison of $\delta\mathbf{F}^{\pm}$ with $\Delta\mathbf{F}^{\pm}$, where the perturbation $\delta\mathbf{q}$ is 10% of the basic state $\mathbf{q}$. Comparison of corresponding perturbation in solar radiation heating rate is shown in Figure 2, with close agreement throughout the vertical column being obtained except for some discrepancy inside the low cloud layer. Even with a perturbation up to 50% of the McClatchey tropical profile $\mathbf{q}$, the perturbation in the solar heating rate from the TLM is still able to capture the structure of the exact finite difference $\Delta\mathbf{F}^{\pm}$ (see Fig. 2b).

Table 1. *Specification of the Clouds used in Verification of the Tangent Linear Model in Section 3 and in Illustration of the Algorithm for Parameter Estimation in Section 4.* In the table, the symbols H, M, and L represent high, middle and low clouds respectively; CAMT the cloud amount; CUVRE the cloud reflectivity for O_3 band, CIRRF the reflectivity and CIRAB the absorptivity for H_2O and C_2O bands; CTOP and CBTM refer to the model levels of cloud top and bottom, where $l=1$ corresponds the TOA and $l=19$ the earth surface

Cloud	CAMT	CUVRF	CIRRF	CIRAB	CTOP	CBTM
H	0.15	0.21	0.21	0.01	9	10
M	0.15	0.48	0.48	0.02	10	15
L	0.45	0.69	0.69	0.03	15	17

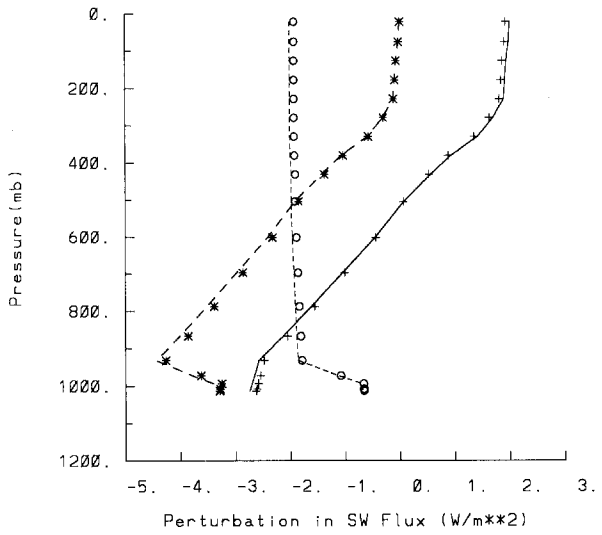

Fig. 1. Comparison of perturbed radiation flux $\delta\mathbf{F}^{\pm}$ from the TLM with corresponding exact finite difference $\Delta\mathbf{F}^{\pm}$, with symbols for $\delta\mathbf{F}^{\pm}$ and lines for $\Delta\mathbf{F}^{\pm}$. The short dash lines and circles are for upward fluxes, solid line and crosses for downward fluxes, and long dash line and stars for net fluxes, respectively. The basic state corresponds to McClatchey tropical profiles and a 10% of perturbation is added to the basic water vapor profile

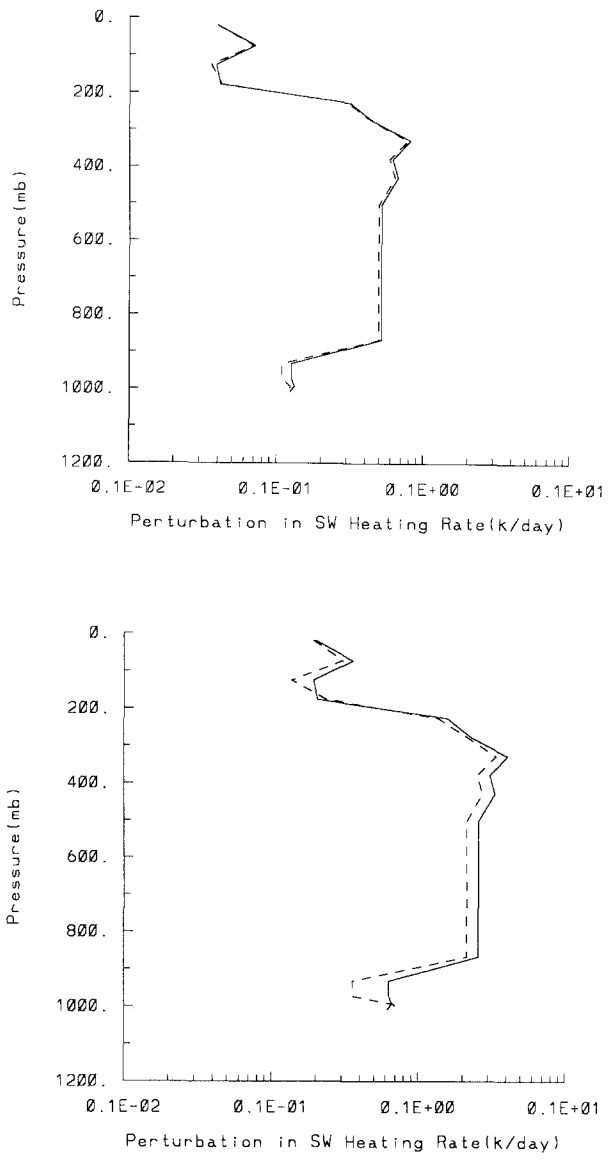

Fig. 2. Comparison of perturbed solar radiation heating rate (represented by dash line) with exact finite difference in the heating rate (solid line). a) for the case shown in Fig. 1. b) for the case of a 50% of perturbation to McClatchey water vapor profile

3.2 The Adjoint Model of the Solar Radiation Codes

To obtain the adjoint model of (20), it is instructive to consider $(\partial \mathbf{F}^{\pm}/\partial \mathbf{q})$ as a linear operator mapping a L-dimensional vector, $\delta \mathbf{q}$ for example, into a $(2L+2)$-dimensional one, $\delta \mathbf{F}^{\pm}$ in this instance. [As before L is taken to be the number of layers in the vertical]. Then its adjoint $(\partial \mathbf{F}^{\pm}/\partial \mathbf{q})^*$ is the transposed expression of $(\partial \mathbf{F}^{\pm}/\partial \mathbf{q})$,

$$(\partial \mathbf{F}^{\pm}/\partial \mathbf{q})^* = \mathscr{P}_4^T \mathscr{P}_3^T \mathscr{P}_2^T \mathscr{P}_1^T \tag{22a}$$

from which we can define the adjoint model as

$$\mathbf{y} = \mathscr{P}_4^T \mathscr{P}_3^T \mathscr{P}_2^T \mathscr{P}_1^T \mathbf{x} \tag{22b}$$

[Here we have denoted an adjoint operator of a linear operator $\mathscr{A}$ by $\mathscr{A}^*$ which is simply the transpose of $\mathscr{A}$, i.e., $\mathscr{A}^* = \mathscr{A}^T$]. Comparing with the TLM (20), we observe that the adjoint model operates in a reverse order, that is, mapping a $(2L+2)$-dimensional vector $\mathbf{x}$ into a vector $\mathbf{y}$ of length L.

The correctness of the adjoint $(\partial \mathbf{F}^{\pm}/\partial \mathbf{q})^*$ can be checked by verifying the equality $\langle \mathbf{y}, (\partial \mathbf{F}^{\pm}/\partial \mathbf{q})\mathbf{x} \rangle = \langle (\partial \mathbf{F}^{\pm}/\partial \mathbf{q})^* \mathbf{y}, \mathbf{x} \rangle$ for arbitrary vectors $\mathbf{x}$ and $\mathbf{y}$ of appropriate length (cf. Navon et al., 1992). Here we take the McClatchey tropical profiles as the basic state, the perturbation to $\mathbf{q}$, $\delta \mathbf{q}$, as the input to the TLM and the resulting perturbation in flux $\delta \mathbf{F}^{\pm}$ as the input to the adjoint model. The aforementioned equality holds to the last digit of machine accuracy (in this case Cray-90).

4. Example of Application

4.1 Parameter Estimation

As the first example of various possible applications of the derived adjoint of the solar radiation routines, we shall outline and illustrate a numerical algorithm for estimating parameter inputs to the solar radiation codes from solar irradiance data.

Parameter estimation with aid of model physics and its corresponding adjoint models has found versatile applications in recent years (Courtier, 1987; Smedstad and O'Brien, 1991; Yu and O'Brien, 1991; Zou et al., 1992; Lardner et al., 1993; Zou and Holloway, 1994; Lardner and Das, 1994). The idea is to treat the estimated input parameters as control variables, by which it is meant that these input parameters are systematically adjusted through an iteration procedure until model outputs are optimally close in a weighted least-square sense to their data counterparts. The optimal estimates are obtained by minimizing a cost function, a measure of the discrepancy between observed data and model counterparts, with respect to a number of distributed parameters serving as control variables.

4.1.1 Cost Function

In the present context, the model physics is given by the solar radiation codes in the NMC spectral

model and the model output is the solar radiation flux $\mathbf{F}^{\pm}$. Clearly, $\mathbf{F}^{\pm}$ is a function of the various inputs to the solar radiation codes, among which is amount of absorbing gases (e.g., water vapor $\mathbf{q}$) and cloud optical properties (e.g., cloud absorptance). Let us introduce a cost function

$$\mathcal{J}(\mathbf{u}) = (1/2)\langle \mathcal{W}(\mathcal{H}\mathcal{A}\mathbf{F}^{\pm}(\mathbf{u}) - \mathcal{A}\mathbf{F}^{\pm ob}), (\mathcal{H}\mathcal{A}\mathbf{F}^{\pm}(\mathbf{u}) - \mathcal{A}\mathbf{F}^{\pm ob})\rangle \tag{23}$$

to measure the quality of estimated parameter inputs $\mathbf{u}$ in terms of the discrepancy between observationally derived data $\mathcal{A}\mathbf{F}^{\pm ob}$ and their model counterpart $\mathcal{A}\mathbf{F}^{\pm}(\mathbf{u})$, where $\langle\ \rangle$ denotes an inner product (i.e., $\langle \mathbf{a}, \mathbf{b}\rangle = \mathbf{b}^T\mathbf{a}$ for vectors $\mathbf{a}$ and $\mathbf{b}$). With this measure, the optimal estimate of $\mathbf{u}$, $\tilde{\mathbf{u}}$, is the one which minimizes $\mathcal{J}(\mathbf{u})$, i.e., $\mathcal{J}(\tilde{\mathbf{u}}) \leqslant \mathcal{J}(\mathbf{u})$.

In the above expression the operator $\mathcal{H}$ represents an interpolation operator which performs spatial (or temporal) interpolation of the model counterpart $A\mathbf{F}^{\pm}(\mathbf{u})$ to the observational points, while $\mathcal{W}$ is a weighting matrix taken as the inverse of error covariance matrix for the data $\mathbf{F}^{\pm ob}$. The operator $\mathcal{A}$ allows one to assess the discrepancy in terms of a desired physical quantity. A natural choice is the radiative flux $\mathbf{F}^{\pm}$ itself, in which case $\mathcal{A}$ corresponds to the unit matrix. Alternatively, one may define the cost function in terms of the solar radiation heating rate $\dot{\mathbf{T}}$, $\dot{\mathbf{T}} \equiv [(\partial T/\partial t)_1, \ldots, (\partial T/\partial t)_2, (\partial T/\partial t)_L]^T$, the final product of the solar radiation codes in the NMC spectral model. In this case $\mathcal{A}$ corresponds to calculation of the radiation heating rate from the upward and downward fluxes $\mathbf{F}^{\pm}$, given by

$$\mathcal{A} = \mathcal{D}\mathcal{C} \tag{24}$$

Here $\mathcal{C}$ performs net flux calculations from the upward and downward fluxes $\mathbf{F}^{\pm}$ and $\mathcal{D}$ carries out divergence operation on the resulting net flux, given respectively by

$$\mathcal{C} = \begin{bmatrix} 1 & -1 & & & & \\ 0 & 0 & 1 & -1 & & \\ & & & & 1 & -1 \end{bmatrix}_{(L+1)\times(2L+2)}$$

and

$$\mathcal{D} = \gamma_d \begin{bmatrix} -1/\Delta p_1 & 1/\Delta P_1 & & \\ & -1/\Delta p_2 & 1/\Delta p_2 & \\ & & & -1/\Delta p_L \quad 1/\Delta p_L \end{bmatrix}_{L\times(L+1)}$$

with γ_d denoting the adiabatic elapse rate.

Prior information on estimated parameters $\mathbf{u}$, $\hat{\mathbf{u}}$, may be incorporated into the cost function by appending a term $\langle \mathcal{W}_{\hat{\mathbf{u}}}(\mathbf{u} - \hat{\mathbf{u}}), (\mathbf{u} - \hat{\mathbf{u}})\rangle$ to (23) (cf. Smedstad and O'Brien, 1991; Zou et al., 1992), where $\mathcal{W}_{\hat{\mathbf{u}}}$ is a weighting matrix. This additional term acting as a quadratic penalty may increase the convexity of $\mathcal{J}(\mathbf{u})$, or can render the Hessian matrix to be positive definite. Either of the two conditions will facilitate convergence of an unconstrained minimization algorithm towards an unique minimum which is an optimal estimate of $\mathbf{u}$, and eliminate spurious secondly minima.

4.1.2 Gradient

The gradient of $\mathcal{J}$ with respect to the estimated parameters, $\nabla_{\mathbf{u}}\mathcal{J}$, is required for minimizing $\mathcal{J}$ using a descent algorithm. To calculate $\nabla_{\mathbf{u}}\mathcal{J}$, let us consider a perturbation $\delta\mathbf{u}$ and the resulting perturbation in the cost function $\delta\mathcal{J}$. It is obvious that $\delta\mathcal{J} = \langle \nabla_{\mathbf{u}}\mathcal{J}, \delta\mathbf{u}\rangle$. On the other hand, taking the first variation of $\mathcal{J}$ with respect to $\mathbf{u}$ we have

$$\delta\mathcal{J} = \langle (\partial\mathbf{F}^{\pm}/\partial\mathbf{u})^*[(\mathcal{W}\mathcal{H}\mathcal{A})^* + (\mathcal{H}\mathcal{A})^*\mathcal{W}](\mathcal{H}\mathcal{A}\mathbf{F}^{\pm} - \mathcal{A}\mathbf{F}^{\pm ob}), \delta\mathbf{u}\rangle$$

where $(\partial\mathbf{F}^{\pm}/\partial\mathbf{u})^*$ is adjoint of the tangent linear operator $(\partial\mathbf{F}^{\pm}/\partial\mathbf{u})$. In case of $\mathbf{u} = \mathbf{q}$, $(\partial\mathbf{F}^{\pm}/\partial\mathbf{u})^*$ is given by (22a); otherwise it can be obtained by some modification to (22) (we shall return to this issue latter). To this end we have

$$\nabla_{\mathbf{u}}\mathcal{J} = (\partial\mathbf{F}^{\pm}/\partial\mathbf{u})^*[(\mathcal{W}\mathcal{H}\mathcal{A})^* + (\mathcal{H}\mathcal{A})^*\mathcal{W}](\mathcal{H}\mathcal{A}\mathbf{F}^{\pm} - \mathcal{A}\mathbf{F}^{\pm ob}) \tag{25}$$

by comparing the two expressions for $\delta\mathbf{u}$. From (25) one can obtain the gradient by a single call to the adjoint codes with the misfit $[(\mathcal{W}\mathcal{H}\mathcal{A})^* + (\mathcal{H}\mathcal{A})^*\mathcal{W}](\mathcal{H}\mathcal{A}\mathbf{F}^{\pm} - \mathcal{A}\mathbf{F}^{\pm ob})$ as its input. This is computationally advantageous compared to the finite difference approach where m executions of the solar radiation codes are required for obtaining $\nabla_{\mathbf{u}}\mathcal{J}$, with m corresponding to the number of distributed parameters to be estimated.

4.1.3 An Algorithm for Parameter Estimation

With the gradient given by (25), an iterative procedure for estimating the parameter inputs to the solar radiation codes from solar irradiance data $\mathbf{F}^{\pm ob}$ may be summarized as follows:

1) set iteration count $m = 0$, make an initial guess at $\mathbf{u}^0$ and calculate $\mathbf{F}^{\pm}(\mathbf{u}^0)$ using the solar

radiation codes and $\nabla_{\mathbf{u}^0}\mathcal{J}$ using the adjoint with initial misfit $[(\mathcal{W}\mathcal{H}\mathcal{A})^* + (\mathcal{H}\mathcal{A})^*\mathcal{W}]$ $(\mathcal{H}\mathcal{A}\mathbf{F}^{\pm}(\mathbf{u}^0) - \mathcal{A}\mathbf{F}^{\pm ob})$ as its input;

2) set $m = m + 1$, check iteration convergence criterion and exit if it is satisfied or continue to next step if not;
3) take one step in the descent direction $\mathbf{d}^m$ to update $\mathbf{u}^{m+1} = \mathbf{u}^m + \lambda\mathbf{d}^m$, where λ is the descent step-size;
4) find out $\mathcal{J}(\mathbf{u}^{m+1})$ and $\nabla_{\mathbf{u}^{m+1}}\mathcal{J}$ as in step 1 but for the updated estimate $\mathbf{u}^{m+1}$, and then go to step 2. The iteration continues until a prescribed convergence criterion is satisfied.

In practice this procedure can be carried out with standard large-scale unconstrained numerical minimization packages (see Zou et al., 1993c) provided that computer codes for evaluating $\mathcal{J}(\mathbf{u}^m)$ and $\nabla_{\mathbf{u}^m}\mathcal{J}$ are made available to the packages. The initial guess, $\mathbf{u}^0$, of the estimated parameters may be made based on a prior knowledge of these parameters (e.g., climatological data).

4.1.4 Numerical Illustrations

To illustrate the algorithm presented above, let us consider the following exercise in which the input parameter to be estimated is water vapor mixing ratio, i.e., $\mathbf{u} = \mathbf{q}$, and the quality of the estimation is measured in terms of the solar radiative heating rate, i.e., $\mathcal{J}(\mathbf{u})$ is given by (23) with $\mathcal{A}$ defined by (24). The flux data $\mathbf{F}^{\pm ob}$ are simulated with the solar radiation codes, corresponding to McClatchey midlatitude summer moisture profile (McClatchey et al., 1971), and assumed to be available at all model levels and perfect (i.e., error-free). The latter renders the operators $\mathcal{H}$ and $\mathcal{W}$ in Eq. (23) immaterial for this illustration, which represents an idealized situation. Care must be exercised to account for paucity and errors of the data in case of real world applications.

Two estimations were carried out, one with a 3-layer cloud and one without. The minimization was performed using the Truncated Newton algorithm as implemented in TNPACK (Schlick and Fogelson, 1992). The initial guess is taken to be 50% of the perturbation to the reference profile. Figure 3 shows the evolution of the cost function and its gradient as a function of number of iterations during the minimization process. It is seen that the estimation for the clear sky case converges successfully within 20 TN iterations.

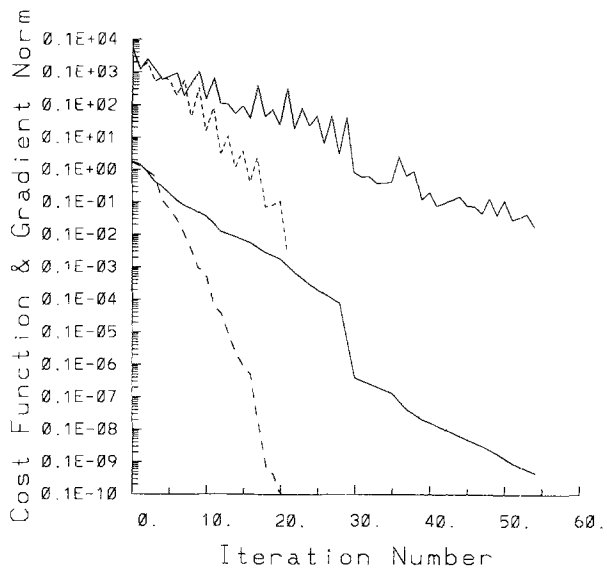

Fig. 3. Cost function and gradient norm evolution as a function of the number of truncated Newton iterations for two parameter estimations, with the solid lines corresponding to the cloudy case and the dashed lines corresponding to the clear sky case, respectively

However, presence of clouds renders the convergence of minimization algorithm more difficult, as evidenced by the relatively larger final cost function value attained for the cloudy case. This situation is also reflected in Fig. 4 which displays estimated profiles of water vapor mixing ratio. As seen here, a close agreement between reference and estimated profiles prevails throughout the vertical column for the clear sky case (see the circles in Fig. 4) whereas a noticeable discrepancy is observed near the 500 mb level when clouds are included (see the crosses in Fig. 4).

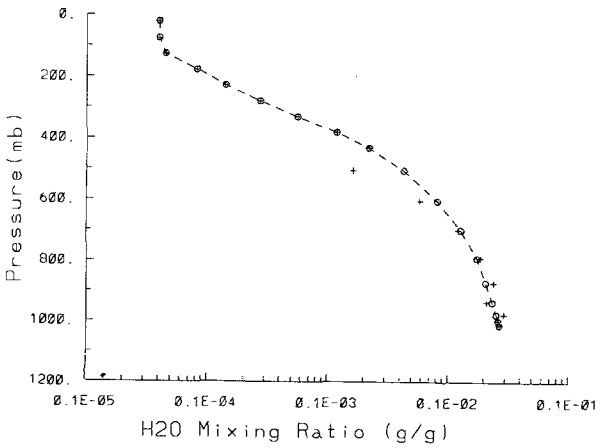

Fig. 4. Optimal estimate of water vapor mixing ratio $\mathbf{q}$ with circles standing for the clear sky case and crosses for the cloudy case. Also shown are the reference value (lines)

It should be pointed out that in practice one has to resort to remotely sensed infrared radiances, TOVS radiances for example, for resolving vertical structure of the water vapor mixing ratio (Thepaut and Moll, 1990; Eyre et al., 1993; Andersson et al., 1994).

4.2 *Adjoint Sensitivity*

Among other potential applications of the TLM of the solar radiation transfer codes and its adjoint is sensitivity analysis of the radiative fluxes (or radiative heating rate) and thus NMC spectral model with respect to the radiation parameterization, cloud specification and other parameter inputs. The existing works following Cacuci (1981a, b), for example by Hall et al. (1982), Hall (1986), Courtier (1987), Rabier et al. (1992), Errico and Vukicevic (1992), and Zou et al. (1993b), have shown how this may be accomplished quantitatively, efficiently and objectively with use of an adjoint model. In fact, all this amounts to calculation of the gradient of a chosen model response, the radiative fluxes (or heating rate) in this case, with respect to various input parameters.

In what follows we shall focus on the downward solar flux at the earth surface F^+_{L+1}, a component of paramount importance for the earth energy budget, and examine its sensitivity with respect to water vapor content at various height (i.e., $\mathbf{q}$ profile). First note that $F^+_{L+1} = \mathbf{e}^T\mathbf{F}^{\pm}$, where $\mathbf{e}$ is a column vector of length $(2L+2)$ with all its entries being equal to zero except for its $(2L+1)$-th entry which is 1, and $\mathbf{F}^{\pm} \equiv [F^+_1, F^-_1, F^+_2, F^-_2, \ldots, F^+_{L+1}, F^-_{L+1}]^T$ as before. Now let the sensitivity be measured in terms of the gradient of F^+_{L+1} with respect to $\mathbf{q}$, $\nabla_{\mathbf{q}} F^+_{L+1}$. As in Section 4b, the gradient (and hence the sensitivity) may be expressed in terms of the adjoint operator $(\partial\mathbf{F}^{\pm}/\partial\mathbf{q})^*$

$$\nabla_{\mathbf{q}} F^+_{L+1} = (\partial\mathbf{F}^{\pm}/\partial\mathbf{q})^*\mathbf{e} \tag{26}$$

where $\mathbf{e}$ serves as an input to the adjoint model. Other sensitivity measures can then readily be computed from (26), among which is the relative sensitivity of F^+_{L+1}

$$RS \equiv \nabla_j F^+_{L+1}/(F^+_{L+1}/q_j), \quad \text{for } j = 1, 2, \ldots, L \tag{27}$$

accounting for the percentage change in F^+_{L+1} for 1% change in the j-th layer water vapor mixing ratio q_j.

Figure 5 shows the relative sensitivity calculated with McClatchey moisture profiles for the tropic, midlatitude summer and winter, and subarctic summer and winter. A number of observations in references to Fig. 5 are in order. First, RS of F^+_{L+1} are found to be negative in all three regions, for both winter and summer and throughout the vertical column. This appears to be consistent with our intuition that less (or more) downward solar radiative flux reaches the earth surface with increased (or reduced) amount of water vapor present along its way down. Second, F^+_{L+1} virtually shows no response to perturbation in water vapor amount in the upper part of the atmosphere, but it becomes increasingly sensitive with increased water vapor downwards and reaches its peak near 850 mb. Further downwards from there, however, the absorption by the ever increased water vapor near the surface tends to become saturated as expected from (3), which accounts for the decreased sensitivity towards the surface. Third, geographically the sensitivity is most pronounced in the tropics and becomes less so towards the poles, whereas seasonally it is larger in summer than in winter.

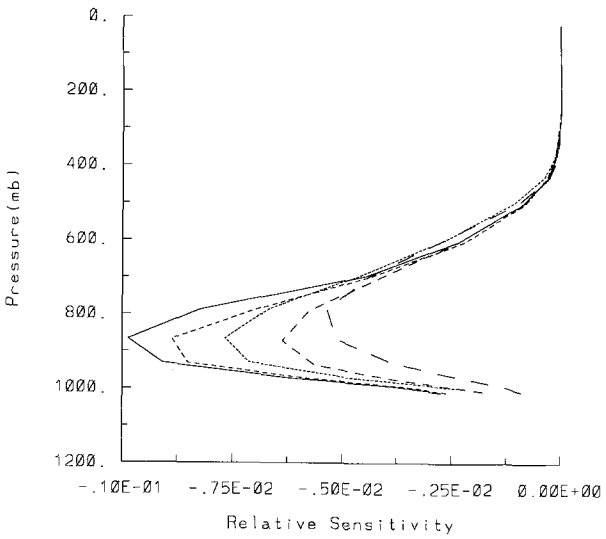

Fig. 5. Relative sensitivity of the downward solar flux at surface with respect to water vapor mixing ratio at various heights. The curves from the left to the right correspond to McClatchey water vapor mixing ratio profiles for the tropic, midlatitude summer, subarctic summer, midlatitude winter and subarctic winter, respectively

5. Summary and Discussion

The adjoint of the solar radiation codes in the NMC spectral model has been derived for the purpose of carrying out 4-D variational data

assimilation, sensitivity analysis and parameter estimation with the above model, while ongoing research on the terrestrial radiation transfer codes will be reported on separately. A verification of validity of the tangent linear model and the correctness of corresponding adjoint has been performed. A numerical algorithm for tuning parameters in the solar radiation codes with aid of the solar radition physics and its corresponding adjoint has been presented and illustrated by considering the problem of estimating water vapor mixing ratio from solar irradiance data. The adjoint has also been applied to sensitivity study of the downward solar radiation flux at the surface with respect to water vapor amount at various heights.

We have focused here on development and verification of the tangent linear model and its corresponding adjoint for the solar radiation codes in the NMC spectral model, and on two possible applications (i.e., parameter estimation and sensitivity study). A host of further questions can and should be raised. A natural concern associated with the adjoint is the recomputation of all the quantities about which to linearize the forward model (see section 3b), a situation typical to any adjoint calculation. Indeed, this may present a computational burden to today's limited computer resources for some applications. Considering the whole range of studies made possible with the adjoint and the gain in computational efficiency as seen from the gradient calculation and sensitivity study in section 4, the effort to derive and run the adjoint might well be worthwhile when compared to what would be required with other approaches (e.g., gradient calculation by the finite difference approach).

We shall conclude by mentioning some of the topics to be considered for future research work.

The tangent linear model (21) and its corresponding adjoint (22) are derived with prognostic variables of the NMC spectral model, namely the water vapor mixing ratio $\mathbf{q}$, as control variables. This is desirable in case of variational data assimilation aiming at obtaining the best analysis of the atmospheric state for subsequent forecast as is the case in Navon et al. (1992) for example. However, it is important to note that any inputs to the solar radiation codes may be treated as control variables in lieu of $\mathbf{q}$ or as additional ones. This may become necessary when one attempts to estimate parameter inputs $\mathbf{u}$ other than $\mathbf{q}$. Some modification to the TLM (21) and its corresponding adjoint (23) may then be required but should be straightforward in principle. For example, if one considers estimating the effective magnification factor for diffuse upward radiation $\bar{M}$ in (6) along with $\mathbf{q}$, i.e., $\mathbf{u} = [\mathbf{q}, \bar{M}]^T$ then the corresponding TLM and its adjoint remain the same as (21) and (22) respectively, except that in this case $\mathscr{P}_4 \equiv (\partial \mathbf{u}^{\pm}/\partial(\mathbf{q}, \bar{M})$.

As in earlier versions of the NMC spectral model (Documentation, 1988), the cloud fractional amount and cloud bottom/top are assumed here to be prescribed by cloud climatology. More realistically, cloud information may be specified as a function of a state vector of the spectral model. In fact, this has already been done with the spectral model (Campana et al., 1990). Specifically, stratiform clouds are diagnosed as a function of relative humidity after Slingo (1980) whereas deep cumulus clouds are specified as a function of convective precipitation rate following the work of Slingo (1987). With these new developments in cloud parameterizations, it is desirable to include the cloud parameters such as cloud fractional amount, as additional control variables in the TLM (21) and its corresponding adjoint (22). This should allows us to examine the interplay among the moisture field, cloud and radiation, especially the sensitivity of radiative processes to cloud characteristics. Of course this extension requires the TLM and its corresponding adjoint of the cloud-diagnosis package for sake of completeness. Development of such tools will constitute a priority task in our future research.

The solar radiation codes in the NMC spectral model have several hard-wired input parameters, some of which have a significant impact on the solar radiative heating rate but are probably among the least known factors in the spectral model. Examples of such parameters are cloud optical properties (e.g., cloud bulk transmissivity and reflectivity). This presents a research opportunity for the future, namely, identifying these cloud optical parameters from data with aid of the physics (i.e., the solar radiative transfer equations) and its corresponding adjoint. The numerical algorithm for performing such a task has been presented in section 4. Solar irradiance data obtained from aircraft measurement during FIRE (Albrecht et al., 1988), or from satellite remote

over time, the small ion concentration is linearly correlated to the density of aerosol particles (Israel, 1971) and hence to the degree of pollution. Ion depletion by attachment to aerosol particles leading to the reduction of conductivity is a process depending strongly on the size distribution of the aerosol particles. Over Athens area there are no heavy industry installations, heating is made exclusively by oil fuel and there is practically no area devoted to agricultural practices. The percentage contribution of each polluting source in smoke and sulfur dioxide over Athens area is as follows (P.E.P.C., 1989):

	Vehicles	Heating	Industry
Smoke	64	17	19
Sulf. dioxide	7	21	72

It is evident that smoke is mainly emitted by vehicles while sulfur dioxide is mainly emitted by industrial installations.

From the above we can deduce that the increased particulate air pollution leads to the decrease of small ion concentration, owing to their becoming, by attachment, large ions (Retalis, 1977). This influence also explains the fact that the large ion concentration at the NOA is much larger than the corresponding small ion concentration (Retalis, 1983). This is a characteristic feature of a heavily polluted area, as is the centre of Athens.

From Tables 1 and 2 it is obvious that when the wind speed increases, positive and negative conductivity increases while the large ion concentration decreases. This is explained as following: The increase in wind speed results in higher dispersion and decrease of large ions and condensation nuclei as opposed to small ions, which are subjected to smaller destruction owing to their recombination. The heavily polluted area around NOA must account for the observed difference between the Mauna Loa results (Cobb, 1968) and those of NOA.

The results of multiple correlation between (a) conductivity and (b) large ion density and air pollution factors are demonstrated in Table 3. The correlation coefficients are considerable mainly during the winter months. The coefficient of determination, which stands for the percentage of variance of large ions due to the cumulative influence of sulfur dioxide, smoke and wind speed is variable being approximately 60%. The corresponding coefficient of determination for the conductivity is 42%.

5. Influence of Air Temperature and Relative Humidity on Conductivity

(a) In order to examine the possible influence of air temperature and relative humidity on the diurnal course of conductivity near the ground for all weather, we proceeded to linear correlation, for each month separately, based on mean hourly values.

Since temperature and relative humidity may exert an indirect influence, we proceeded to cross correlation with a lag time 0, 1, 2, and 3 hours (Table 4).

The contribution of these elements to the diurnal variation of the conductivity is considerable, especially during the warm months (April–September). Air temperature is positively while the relative humidity is negatively correlated to conductivity (owing perhaps to its inverse temperature dependence). The greatest influence is observed after a time lag of 3 hours.

These results are similar to those of D. Retalis and J. Zambakas (1975), who examined the influence of air temperature and relative humidity on small ion concentration variation except for a difference in the time lag. The corresponding influ-

Table 3. *Monthly Values of Multiple Correlation Coefficient Between Conductivity* (positive $R_{(\lambda+)}$ and negative $R_{(\lambda-)}$), *Large Ions* (positive $R_{(N+)}$ and negative $R_{(N-)}$) *and (1) Smoke, (2) Sulfur Dioxide and (3) Wind Speed*

	J	F	M	A	M	J	J	A	S	O	N	D
$R_{(\lambda+)}$	0.742	0.748	0.428	0.483	0.722	0.507	0.571	0.692	0.401	0.692	0.777	0.699
$R_{(\lambda-)}$	0.806	0.829	0.527	0.401	0.764	0.391	0.574	0.612	0.694	0.424	0.817	0.813
$R_{(N+)}$	0.858	0.745	0.765	0.709	0.656	0.736	0.843	0.897	0.707	0.597	0.866	0.894
$R_{(N-)}$	0.867	0.773	0.549	0.855	0.762	0.341	0.768	0.608	0.890	0.932	0.891	0.903

Rabier, F., Courtier, P., Talagrand, O., 1992: An application of adjoint models to sensitivity analysis. *Beitr. Phys. Atmos.*, **65**, 177–192.

Sasamori, T., London, J., Hoyt, D., 1972: Radiation budget of the southern hemisphere. *Meteorological Monographs*, **13**, 9–23.

Schlick, T., Fogelson, A., 1992: TNPACK-A truncated Newton minimization package for large-scale problems, I. Algorithms and usage, II. Implementation examples. *ACM Trans. Math Software*, **18**, 46–111.

Slingo, J. M., 1980: A cloud parameterization scheme derived from GATE data for use with a numerical model. *Quart. J. Roy. Meteor. Soc.*, **106**, 747–770.

Slingo, J. M., 1987: The development and verification of a cloud prediction scheme for the ECMWF. *Quart. J. Roy. Meteor. Soc.*, **113**, 899–927

Smedstad, O. M., O'Brien, J. J., 1991: Variational data assimilation and parameter estimation in the equatorial Pacific Ocean. *Prog. Oceanogr.*, **26**, 179–241.

Thepaut, J. N., Moll, P., 1990: Variational inversion of simulated TOVS radiances using the adjoint technique. *Quart. J. Roy. Meteor. Soc.*, **116**, 1425–1448.

Vukicevic, T., Errico, R. M., 1993: Linearization and adjoint of parameterized moist diabatic process. *Tellus*, **44A**, 273–296.

Wu, W. S., Derber, J. C., 1994: Inclusion of SSM/I precipitable water observations in the NMC spectral statistical interpolation analysis system. in Proc. of the Tenth Conference on Numerical Weather Predication, held in Portland, Oregon, July 18–22, 1994. 190–191. pp. 640.

Zou, J., Holloway, G., 1994: Improving steady-state fit of dynamics to data using adjoint equation with gradient preconditioning. *Mon. Wea. Rev.*, **123**/1, 199–211.

Zou, X., Navon, I. M., 1994a: Variational data assimilation: some aspects of theory and applications. In *Environmental Modeling Vol II: Computer Methods and Software for Simulating Environmental Pollution and its Adverse Effects*. Boston: Computational Mechanics Publications, 350pp.

Zou, X., Derber, J. C., Sela, J. G., Navon, I. M., 1994b: Variational data assimilation with physical processes using the NMC spectral model. Presented at the Tenth Conference on Numerical Weather Prediction, held in Portland, Oregon, July 18–22, 1994.

Zou, X., Navon, I. M., Sela, J., 1993a: Control of gravitational oscillations in variational data assimilation. *Mon. Wea. Rev.*, **121**, 272–289.

Zou, X., Navon, I. M., Sela, J., 1993b: Variational data assimilation with moist threshold processes using the NMC spectral model. *Tellus*, **45A**, 370–387.

Zou, X., Navon, I. M., Berger, M., Phua, K. H., Schlick, T., Le Dimet, F. X., 1993c: Numerical experiences with limited-memory quasi-Newton and truncated Newton methods. *Siam J. Optimization*, **3**, 582–608.

Zou, X., Navon, I. M., Barcilon, A., Whittaker, J., Cacuci, D., 1993d: An adjoint sensitivity study of blocking in a two-layer isentropic model. *Mon. Wea. Rev.*, **121**, 2833–2857.

Zou, X., Navon, I. M., Le-Dimet, F. X., 1992: An optimal nudging data assimilation using parameter estimation. *Quart. J. Roy. Meteor. Soc.*, **118**, 1163–1186.

Zupanski, D., 1993: The effects of discontinuities in the Betts-Miller cumulus convection scheme on four-dimensional data assimilation, *Tellus*, **45A**, 511–524.

Yu, L., O'Brien, J. J., 1991: Variational estimation of the wind stress drag coefficient and oceanic eddy viscosity profile. *J. Phys. Oceanogr.*, **21**, 709–719.

Authors' addresses: Jieping Zou, Supercomputer Computational Research Institute, Florida State University, Tallahassee, FL 32306, U.S.A.; I. M. Navon, Department of Mathematics and SCRI and GFDI Faculty Associate, Florida State University, Tallahassee, Florida, U.S.A.